

# Tracking Radiometer Calibration Stability Using Three-Point Onboard Calibration

Mustafa Aksoy

Department of Electrical and Computer Engineering  
University at Albany, SUNY  
Albany, NY, USA

Paul E. Racette

NASA Goddard Space Flight Center  
Greenbelt, MD, USA

**Abstract**— Absolute calibration of radiometers is implemented onboard using one hot and one cold external calibration targets. However, two-point calibration methods are unable to differentiate calibration drifts and associated errors from fluctuations in receiver gain and offset. This paper investigates the use of onboard three-point calibration algorithm for microwave radiometers to track calibration drifts and characterize associated errors in Earth and Space measurements of the radiometer.

**Keywords**—microwave radiometer; calibration; stability

## I. INTRODUCTION

Microwave radiometers have been used to measure important geophysical parameters over extended time periods to examine variations in the Earth System. Detecting small, long term trends, such as the temperature change in the troposphere which has been measured as 0.14-0.18 K/decade since 1979 [1], accurately via microwave radiometers requires precise absolute calibration and increased stability. Thus, it is critical to track calibration drifts, and correct radiometer measurements when calibration errors occur.

Absolute calibration of microwave radiometers is usually performed onboard by observing one hot and one cold target to compute the receiver gain and offset, i.e. two-point algorithm [2]. However, two-point algorithms are inadequate to detect drifts in absolute calibration as they cannot distinguish calibration errors from receiver gain fluctuations. This paper aims to address this issue by presenting a three-point onboard calibration method which offers the means to quantify calibration drifts and associated measurement errors.

## II. LINEAR CALIBRATION

The general n-point linear radiometer calibration model is given as [3]:

$$\widehat{T}_m = (v_m - \langle v_i \rangle_n) \frac{\sum_{i=1}^n (v_i - \langle v_i \rangle_n) T_i}{\sum_{i=1}^n (v_i - \langle v_i \rangle_n)^2} + \langle T_i \rangle_n \quad (1)$$

where  $\widehat{T}_m$  is the estimated measurand temperature,  $v_m$  is measurand voltage counts,  $v_i$  is the  $i^{\text{th}}$  calibration voltage counts,  $T_i$  is the  $i^{\text{th}}$  calibration temperature measurement, and  $\langle \cdot \rangle_n$  represents the ensemble average. The uncertainty associated with the estimated measurand temperature is also defined as:

$$\sigma_{\widehat{T}_m}^2 = \sigma_{T_m}^2 + \frac{\sum_{i=1}^n (\sigma_{T_i}^2 + \sigma_{\bar{T}_i}^2)}{n^2} + \frac{(\langle T_m - \langle \bar{T}_i \rangle_n \rangle^2 \sum_{i=1}^n (\bar{T}_i - \langle \bar{T}_i \rangle_n)^2 (\sigma_{T_i}^2 + \sigma_{\bar{T}_i}^2))}{(\sum_{i=1}^n (\bar{T}_i - \langle \bar{T}_i \rangle_n)^2)^2} + \frac{2(\langle T_m - \langle \bar{T}_i \rangle_n \rangle \sum_{i=1}^n (\bar{T}_i - \langle \bar{T}_i \rangle_n) (\sigma_{T_i}^2 + \sigma_{\bar{T}_i}^2))}{n \sum_{i=1}^n (\bar{T}_i - \langle \bar{T}_i \rangle_n)^2} \quad (2)$$

where  $\sigma_{\widehat{T}_m}$  is the uncertainty associated with the measurand temperature estimate,  $\sigma_{T_m}$  is the measurand resolution,  $\sigma_{T_i}$  is the  $i^{\text{th}}$  calibration resolution,  $\bar{T}_i$  is the mean temperature of the  $i^{\text{th}}$  calibration target,  $\sigma_{\bar{T}_i}$  is the uncertainty associated with the  $i^{\text{th}}$  calibration temperature knowledge, and  $T_m$  is the observed measurand temperature.

The following sections discuss a linear radiometer defined by equations (1) and (2), thus nonlinear effects are ignored.

## III. 2-POINT ONBOARD CALIBRATION

Consider a radiometer measuring the atmospheric temperature wherein 2.7 K cold space and a 300 K warm blackbody target are used for absolute onboard calibration as shown in Figure 1. Since the atmospheric temperature is unknown, changes in voltage counts due to calibration drifts and receiver gain and offset fluctuations cannot be separated.

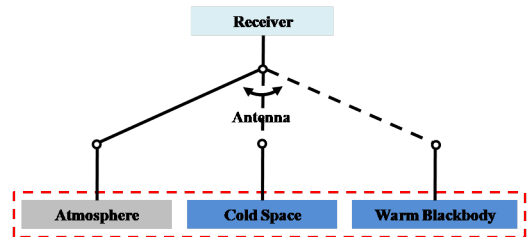


Fig. 1. Two-point onboard calibration configuration. Atmospheric measurements are calibrated using cold space and warm blackbody targets.

Assuming 1-second integration time, 500 K system temperature, and 100 MHz receiver bandwidth; measurement errors due to calibration drifts are shown in Figure 2 when the radiometer is observing 250 K brightness temperature (Note that the radiometric resolution of the atmospheric measurements is 0.075 K with this configuration). Detectability of these errors is defined as the ratio of the bias due to the error to the uncertainty in the measurement:

$$Detectability = \frac{\langle \hat{T}_m \rangle - \langle T_m \rangle}{\sigma_{\hat{T}_m}} \quad (3)$$

and the error is considered detectable if the detectability is larger than 1.

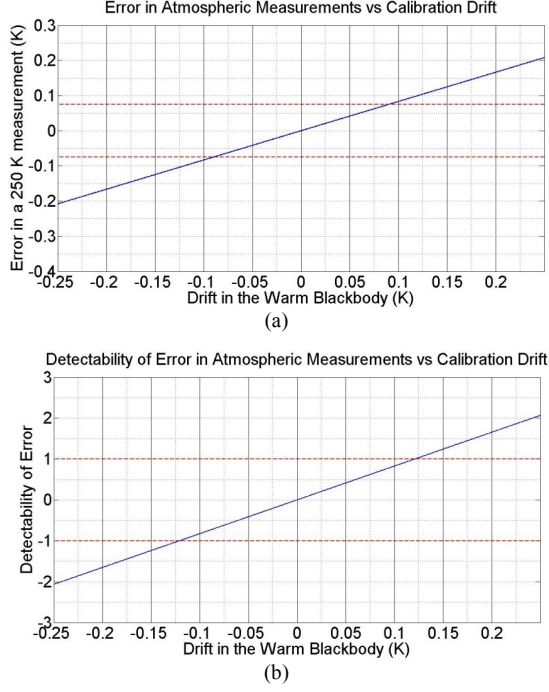


Fig. 2. (a) Errors in 250 K Atmospheric measurements due to drifts in 300 K warm blackbody measurements. (b) Detectability of the errors.

#### IV. 3-POINT ONBOARD CALIBRATION

When a third blackbody calibration target is added to the radiometer, calibration measurements can be used as references to track onboard calibration drifts [4]. One way to achieve this goal is to operate the radiometer in two modes:

##### A. Measurement Mode

In the measurement mode, three calibration targets are used to calibrate the measurand, i.e. the atmospheric measurements as shown in Figure 3. Similar to Figure 2 in Section III, Figure 4 depicts the measurement errors and their detectabilities as functions of calibration drifts in warm blackbody targets when a 250 K atmospheric scene is observed. Note that the temperature of the additional calibration target is assumed to be 290 K.

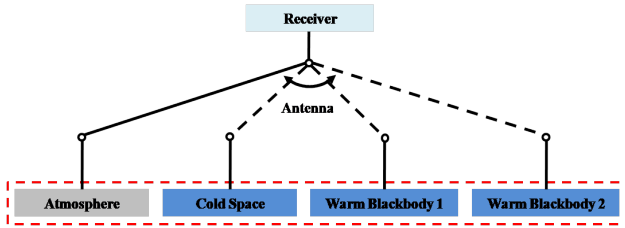


Fig. 3. Radiometer with three calibration targets in measurement mode. Atmospheric measurements are calibrated using cold space and two warm blackbody targets.

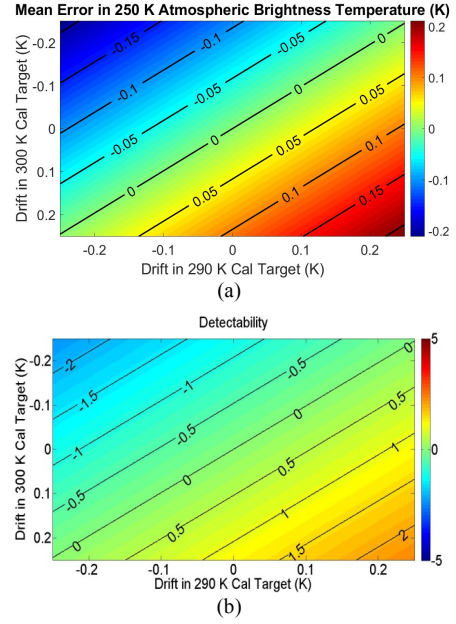


Fig. 4. (a) Errors in 250 K Atmospheric measurements due to drifts in 290 K and 300 K warm blackbody measurements during the measurement mode. (b) Detectability of the errors.

##### B. Calibration Validation Mode

In the calibration validation mode, the measurand is not observed. Instead, measurements from two calibration targets are used to calibrate the third calibration target measurements. Since all calibration temperatures are known, measurement errors in this mode can be associated with calibration drifts. Figure 5 demonstrates the radiometer configuration in this mode. Figure 6, on the other hand, shows the measurement errors and associated detectabilities when two blackbody targets are used to calibrate the cold sky measurements to validate the accuracy of the radiometer calibration.

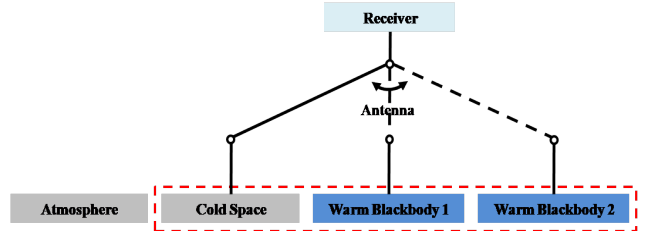


Fig. 5. Radiometer with three calibration targets in calibration validation mode. Atmosphere is not measured, cold space is calibrated using two blackbody targets.

#### V. ERROR ANALYSIS

Detectability of error information shown in Figures 4 and 6 can be combined into one “calibration error analysis” (CEA) diagram as illustrated in Figure 7. CEA diagrams show errors associated with calibration drifts and indicate the possibility of four scenarios:

1. Calibration drifts cause detectable errors in cold space measurements and lead to significant errors in atmospheric measurements (blue region in Figure 7).

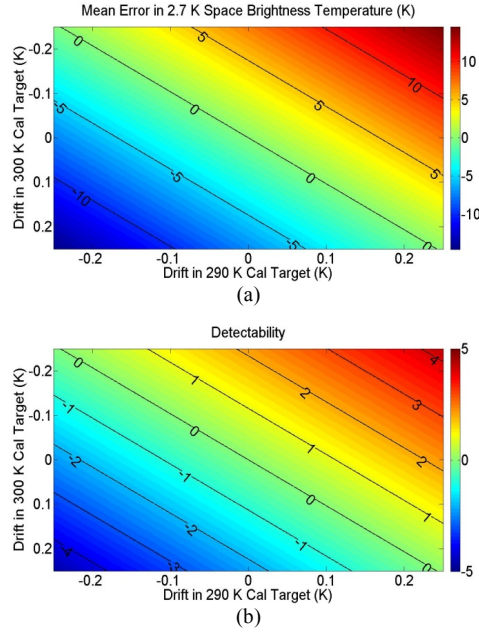


Fig. 6. (a) Errors in 2.7 K Cold Space measurements due to drifts in 290 K and 300 K warm blackbody measurements during the calibration validation mode. (b) Detectability of the errors.

2. Calibration drifts induce significant errors in cold space measurements but have undetectable effects on atmospheric measurements (yellow region in Figure 7).
3. Calibration drifts result in no/undetectable errors in cold space measurements but cause significant errors in atmospheric observations (red region in Figure 7).
4. Calibration drifts result in no/undetectable errors in cold space and atmospheric measurements (white region in Figure 7).

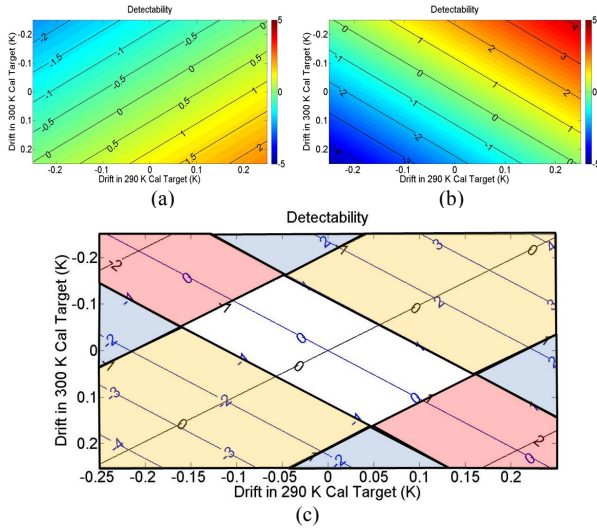


Fig. 7. (a) Detectabilities from the measurement mode (Figure 4-b). (b) Detectabilities from the calibration validation mode (Figure 6-b). (c) Calibration error analysis (CEA) diagram combining (a) and (b).

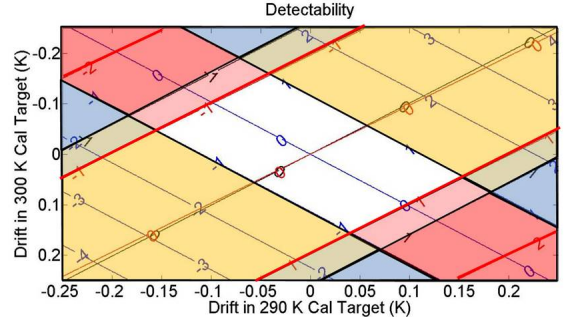


Fig. 8. CEA diagram when the true atmospheric temperature is 180 K (black lines) and 280 K (red lines). Notice that blue lines representing the detectabilities from the calibration validation mode are independent of the atmospheric temperature.

Figure 8 shows the change in the CEA diagram for the radiometer system discussed thereof as the atmospheric temperature varies from 180 K to 280 K. The calibration validation information is independent of the atmospheric temperature, thus remains constant. However, once the atmospheric temperature is roughly estimated, an approximate CEA diagram can be created.

Any error identified in the calibration validation mode corresponds a line on the CEA diagram, thus provide information about the possible errors in estimated measurand temperatures and detectabilities of those errors.

Figure 9 shows an example in which calibration drifts lead to a 7.5 K calibration error detected in the calibration and validation mode. Although the error is significant, the corresponding line in the CEA diagram is mostly in the yellow region, and it can be said that the effects of the calibration drift on the atmospheric temperature estimations are minimal. There is a slight chance of having a detectable error in atmospheric measurements only if the atmosphere is warm, i.e. its true temperature is close to 280 K.

## VI. CONCLUSIONS AND DISCUSSION

Assuming a linear system, this paper presents a three-point onboard calibration scheme via calibration error analysis (CEA) diagrams which provides means to quantify the calibration drifts and associated measurement errors. However, measuring the exact magnitude of errors and the ways to correct them requires further investigations.

Adjusting calibration temperatures and radiometer integration times to reshaping the regions in the CEA diagrams to minimize the impacts of calibration drifts will be examined in future studies. Moreover, a similar study will be carried out for non-linear systems and a cost analysis for having an additional calibration target will be done.

Note that three or more calibration targets are usually used in pre-launch characterization of radiometers to test their linearity and stability [5]-[6]. However, this study discusses an onboard implementation where the errors in unknown geophysical measurements are characterized using CEA diagrams.

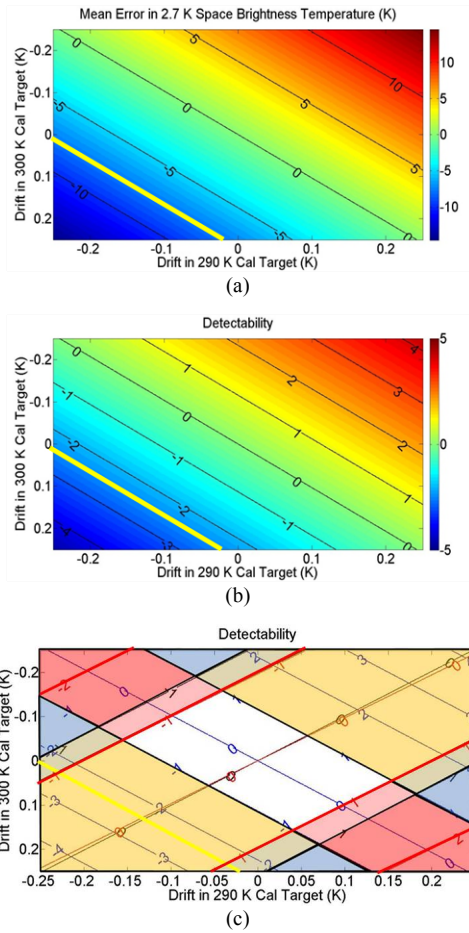


Fig. 9. (a) 7.5 K error detected in cold space measurements during the calibration validation mode. (b) Detectability of the error. (c) The error in the CEA diagram. Notice that if the atmosphere is cold, the entire line is within the yellow region where the impact of the calibration drift on the atmospheric measurements is minimal during the measurement mode.

## REFERENCES

- [1] Foster, G. and Rahmstorf, S., 2011. Global temperature evolution 1979–2010. *Environmental Research Letters*, 6(4), p.044022.
- [2] Ruf, C.S., 2000. Detection of calibration drifts in spaceborne microwave radiometers using a vicarious cold reference. *IEEE Transactions on Geoscience and Remote Sensing*, 38(1), pp.44-52.
- [3] Racette, P. and Lang, R.H., 2005. Radiometer design analysis based upon measurement uncertainty. *Radio science*, 40(5).
- [4] Aksoy, M. and Racette, P.E., 2017, July. Tracking calibration stability in climate monitoring microwave radiometers using onboard 3-point calibration. In *Geoscience and Remote Sensing Symposium (IGARSS), 2017 IEEE International* (pp. 2118-2120). IEEE.
- [5] Saunders, R.W., Hewison, T.J., Stringer, S.J. and Atkinson, N.C., 1995. The radiometric characterization of AMSU-B. *IEEE Transactions on microwave theory and techniques*, 43(4), pp.760-771.
- [6] Draper, D.W., Newell, D.A., McKague, D.S. and Piepmeier, J.R., 2015. Assessing calibration stability using the Global Precipitation Measurement (GPM) Microwave Imager (GMI) noise diodes. *IEEE Journal of Selected Topics in Applied Earth Observations and Remote Sensing*, 8(9), pp.4239-4247.



# Tracking Radiometer Calibration Stability Using Three-Point Onboard Calibration

Mustafa Aksoy<sup>1</sup> and Paul E. Racette<sup>2</sup>

<sup>1</sup> University at Albany, SUNY

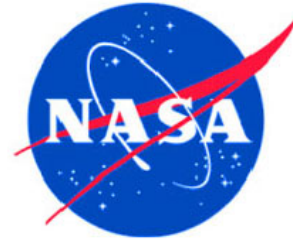
<sup>2</sup> NASA Goddard Space Flight Center

MicroRad 2018

March 30, 2018



# Motivation



Microwave radiometers have been used to measure important geophysical parameters over extended time periods to examine variations in the Earth System.

- Detecting small, long term trends (e.g. temperature change in the troposphere has been measured as 0.14-0.18 K/decade since 1979 [1]), accurately via microwave radiometers requires precise absolute calibration and increased stability.
- It is critical to track calibration drifts, and correct radiometer measurements when calibration errors occur.

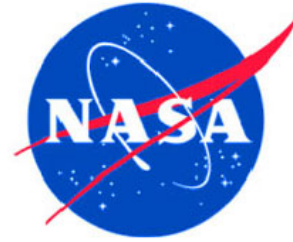
Absolute calibration of microwave radiometers is usually performed onboard by observing one hot and one cold target to compute the receiver gain and offset, i.e. two-point algorithm.

- However, two-point algorithms are inadequate to detect drifts in absolute calibration as they cannot distinguish calibration errors from receiver gain fluctuations.

Can three-point calibration offer the means to quantify calibration drifts and associated measurement errors?



# Linear Calibration



The general n-point linear radiometer calibration model:

$$\widehat{T}_m = (v_m - \langle v_i \rangle_n) \frac{\sum_{i=1}^n (v_i - \langle v_i \rangle_n) T_i}{\sum_{i=1}^n (v_i - \langle v_i \rangle_n)^2} + \langle T_i \rangle_n$$

$\widehat{T}_m$  : Estimated measurand temperature       $v_m$  : Measurand voltage counts

$T_i$  :  $i^{\text{th}}$  calibration temperature measurement       $v_i$  :  $i^{\text{th}}$  calibration voltage counts

$\langle \cdot \rangle_n$  : the ensemble average

The uncertainty associated with the estimated measurand temperature:

$$\sigma_{\widehat{T}_m}^2 = \sigma_{T_m}^2 + \frac{\sum_{i=1}^n (\sigma_{T_i}^2 + \sigma_{\bar{T}_i}^2)}{n^2} + \frac{(T_m - \langle \bar{T}_i \rangle_n)^2 \sum_{i=1}^n (\bar{T}_i - \langle \bar{T}_i \rangle_n)^2 (\sigma_{T_i}^2 + \sigma_{\bar{T}_i}^2)}{(\sum_{i=1}^n (\bar{T}_i - \langle \bar{T}_i \rangle_n)^2)^2} + \frac{2(T_m - \langle \bar{T}_i \rangle_n) \sum_{i=1}^n (\bar{T}_i - \langle \bar{T}_i \rangle_n) (\sigma_{T_i}^2 + \sigma_{\bar{T}_i}^2)}{n \sum_{i=1}^n (\bar{T}_i - \langle \bar{T}_i \rangle_n)^2}$$

$\sigma_{\widehat{T}_m}$  : Uncertainty in the measurand temperature estimate       $\sigma_{T_m}$  : Measurand resolution

$\bar{T}_i$  : Mean temperature of the  $i^{\text{th}}$  calibration target       $\sigma_{T_i}$  :  $i^{\text{th}}$  calibration resolution

$T_m$  : Observed measurand temperature

$\sigma_{\bar{T}_i}$  : Uncertainty associated with the  $i^{\text{th}}$  calibration temperature knowledge



# Two-Point Calibration

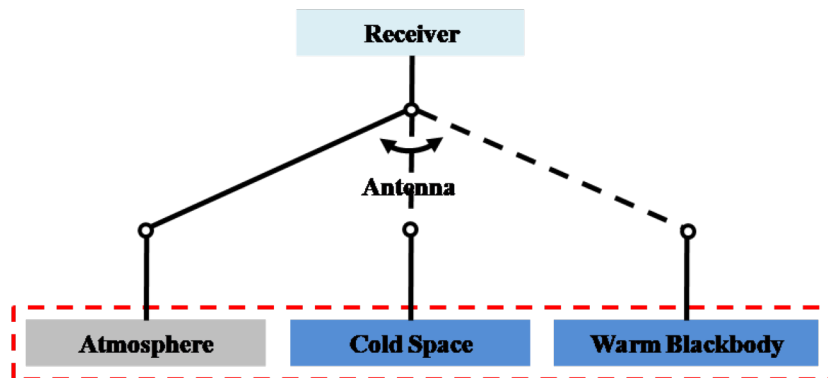
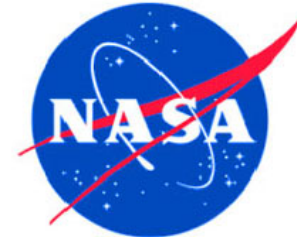


Fig. 1. Two-point onboard calibration configuration. Atmospheric measurements are calibrated using cold space and warm blackbody targets.

Consider a radiometer measuring 250 K atmospheric temperature wherein 2.7 K cold space and a 300 K warm blackbody target are used for absolute onboard calibration as shown in Figure 1.

Assume 1-second integration time, 500 K system temperature, and 100 MHz receiver bandwidth.

$$Detectability = \frac{\langle \widehat{T}_m \rangle - \langle T_m \rangle}{\sigma_{\widehat{T}_m}}$$

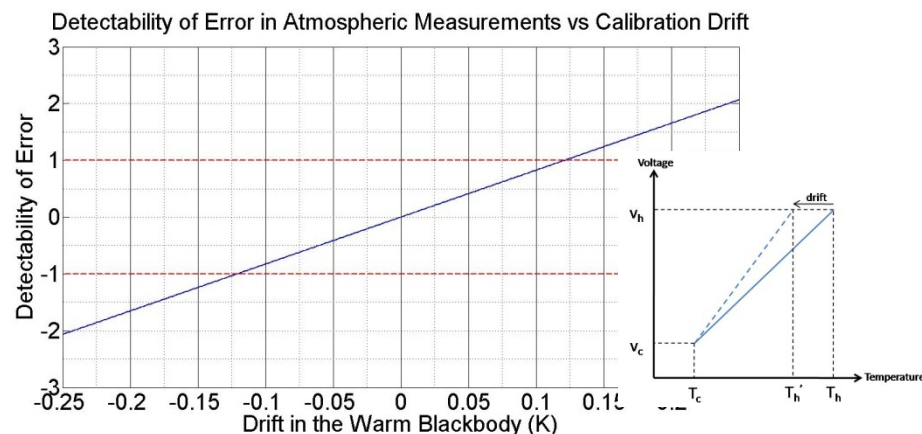
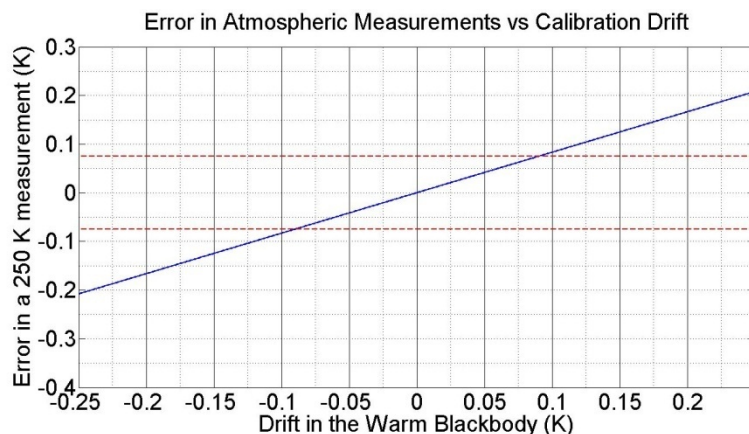
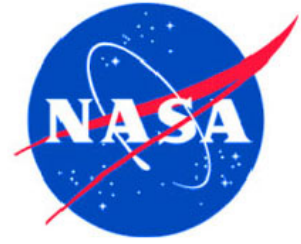


Fig. 2. (left) Errors in 250 K Atmospheric measurements due to drifts in 300 K warm blackbody measurements. (right) Detectability of the errors.





# Three-Point Calibration



When a third blackbody calibration target is added to the radiometer, calibration measurements can be used as references to track onboard calibration drifts. One way to achieve this goal is to operate the radiometer in two modes:

## Measurement Mode:

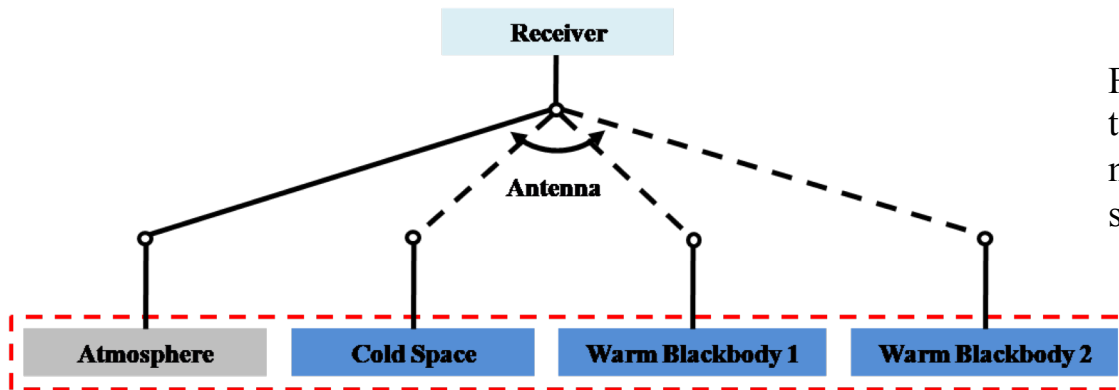


Fig. 3. Radiometer with three calibration targets in measurement mode. Atmospheric measurements are calibrated using cold space and two warm blackbody targets.

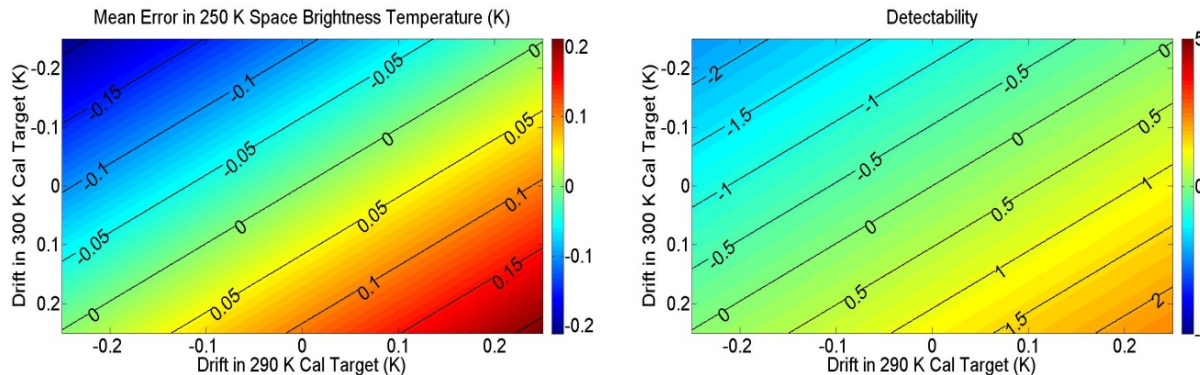
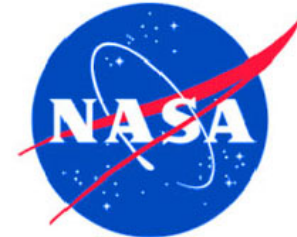


Fig. 4. (left) Errors in 250 K Atmospheric measurements due to drifts in 290 K and 300 K warm blackbody measurements during the measurement mode. (right) Detectability of the errors.



# Three-Point Calibration



## Calibration-Validation Mode:

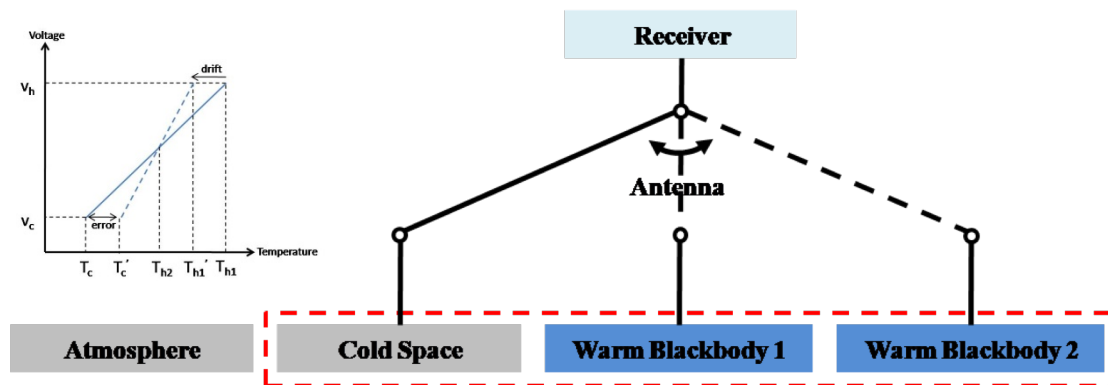


Fig. 5. Radiometer with three calibration targets in calibration validation mode. Atmosphere is not measured, cold space is calibrated using two blackbody targets.

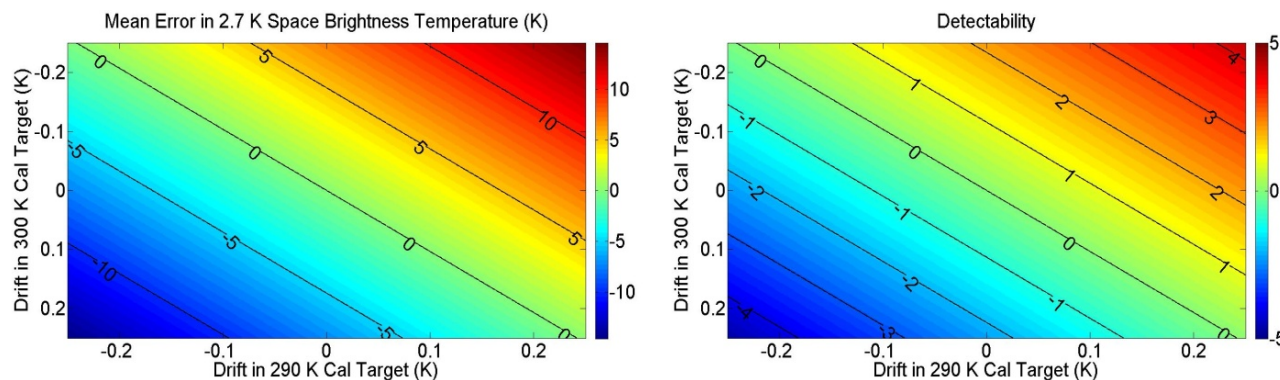


Fig. 6. (left) Errors in 2.7 K Cold Space measurements due to drifts in 290 K and 300 K warm blackbody measurements during the calibration validation mode. (right) Detectability of the errors.

Information from two modes can be displayed in one “Calibration Error Analysis” (CEA) diagram.



# Calibration Error Analysis

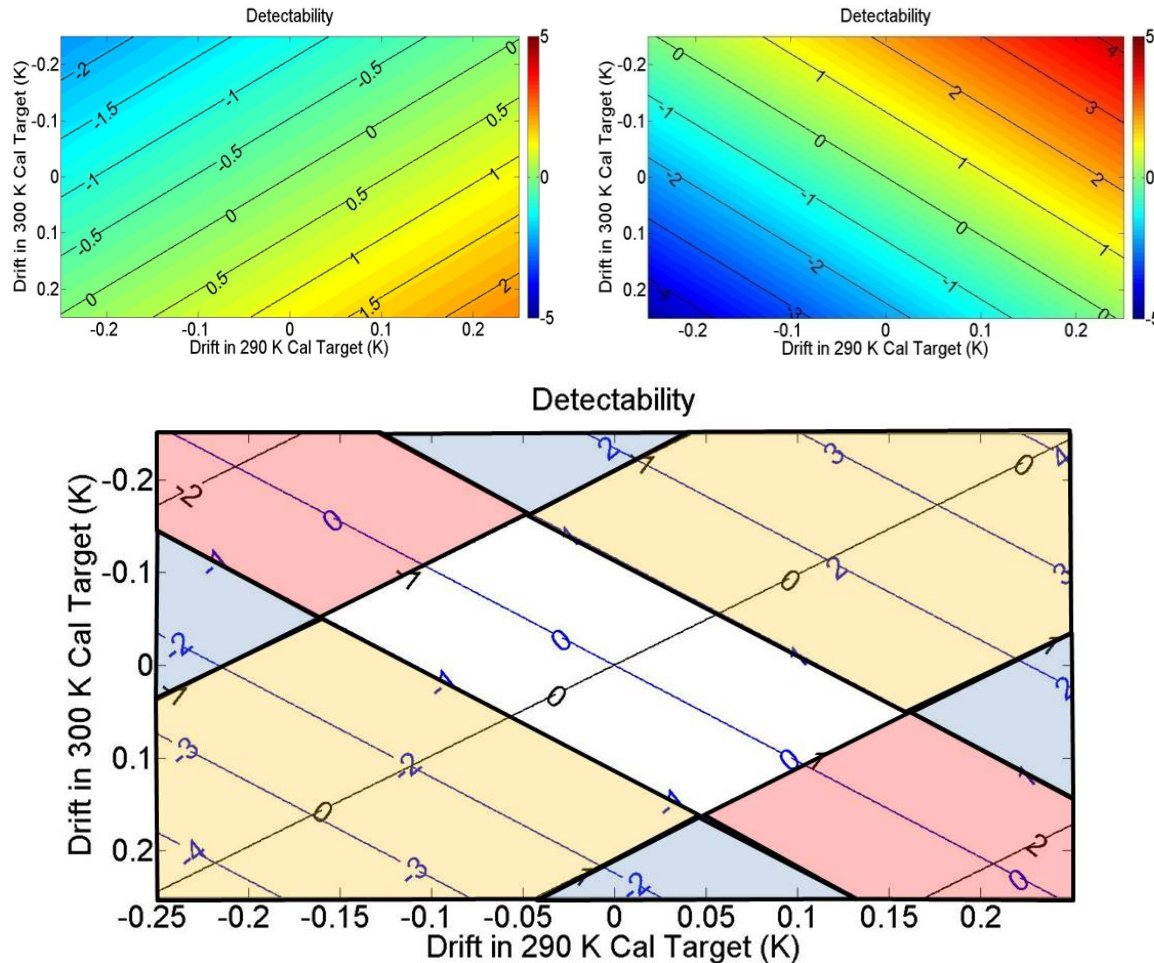
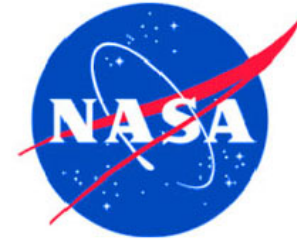


Fig. 7. (top-left) Detectabilities from the measurement mode. (top-right) Detectabilities from the calibration validation mode. (bottom) Calibration error analysis (CEA) diagram combining them.

1. Calibration drifts cause detectable errors in cold space measurements and lead to significant errors in atmospheric measurements (**blue** region).
2. Calibration drifts induce significant errors in cold space measurements but have undetectable effects on atmospheric measurements (**yellow** region).
3. Calibration drifts result in no/undetectable errors in cold space measurements but cause significant errors in atmospheric observations (**red** region).
4. Calibration drifts result in no/undetectable errors in cold space and atmospheric measurements (white region).



# Calibration Error Analysis

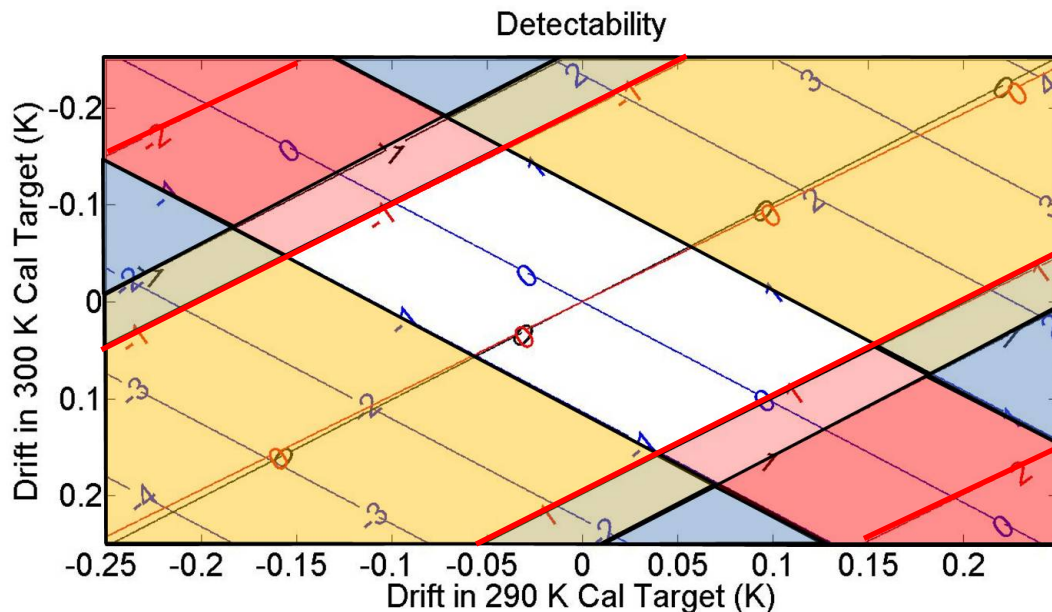
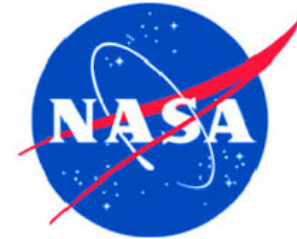


Fig. 8. CEA diagram when the true atmospheric temperature is 180 K (black lines) and 280 K (red lines). Notice that blue lines representing the detectabilities from the calibration validation mode are independent of the atmospheric temperature.

The change in the CEA diagram as the atmospheric temperature varies from 180 K to 280 K. The Cal-Val information is independent of the atmospheric temperature, thus remains constant.

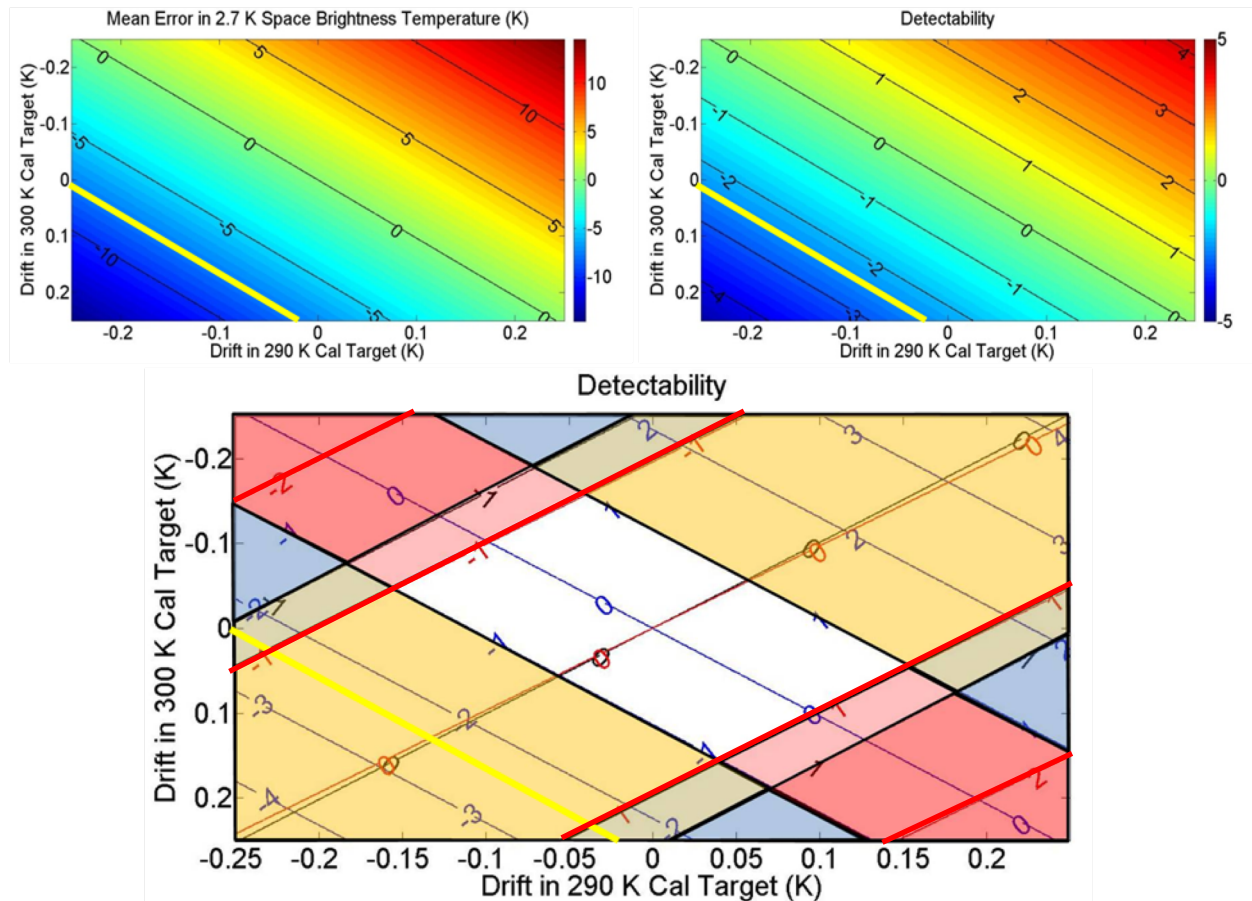
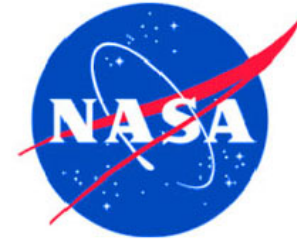
If the atmospheric temperature is roughly estimated, an approximate CEA diagram can be created.

Any error identified in the calibration validation mode corresponds a line on the CEA diagram, thus provide information about the possible errors in estimated measurand temperatures and detectabilities of those errors.





# Calibration Error Analysis



## Example:

-7.5 K calibration error detected in the calibration and validation mode due to calibration drifts.

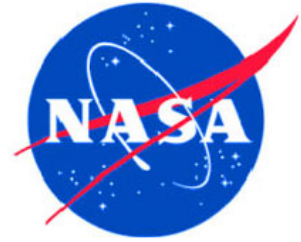
Although the error is significant, the line associated with it in the CEA diagram is mostly in the yellow region, which means the effects of the calibration drift on the atmospheric temperature estimations are minimal.

Fig. 9. (top-left) 7.5 K error detected in cold space measurements during the calibration validation mode. (top-right) Detectability of the error. (bottom) The error in the CEA diagram. Notice that if the atmosphere is cold, the entire line is within the yellow region where the impact of the calibration drift on the atmospheric measurements is minimal during the measurement mode.





# Conclusions and Future Plan



- Assuming a linear system, this preliminary study presents a three-point onboard calibration scheme via calibration error analysis (CEA) diagrams which provides means to quantify the calibration drifts and associated measurement errors.
- However, measuring the exact magnitude of errors and the ways to correct them requires further investigations.
- Adjusting calibration temperatures and radiometer integration times to reshaping the regions in the CEA diagrams to minimize the impacts of calibration drifts will be examined in future studies.
- Moreover, a similar study will be carried out for non-linear systems and a cost analysis for having an additional calibration target will be done.

**Thank you...**

**Questions?**